Electrochimica Acta 55 (2010) 6239–6247

Contents lists available at ScienceDirect

Electrochimica Acta

journal homepage: www.elsevier.com/locate/electacta

Electrochemical impedance studies of chitosan-modified electrodes for application in electrochemical sensors and biosensors

Rasa Pauliukaite[a], Mariana E. Ghica[a], Orlando Fatibello-Filho[a,b], Christopher M.A. Brett[a,*]

[a] Departamento de Química, Faculdade de Ciências e Tecnologia, Universidade de Coimbra, 3004-535 Coimbra, Portugal
[b] Departamento de Química, Universidade Federal de São Carlos, C.P. 676, 13560-970 São Carlos, SP, Brazil

ARTICLE INFO

Article history:
Received 14 June 2009
Received in revised form
11 September 2009
Accepted 18 September 2009
Available online 23 September 2009

Keywords:
Chitosan
Electrochemical impedance spectroscopy
Crosslinking agents
Functionalised carbon nanotubes
Sensor and biosensor

ABSTRACT

Graphite-epoxy resin composite (GrEC) electrodes were modified with chitosan (Chit) films and characterised using electrochemical impedance spectroscopy (EIS). Several film modifications were made using different crosslinking agents: glutaraldehyde (GA), glyoxal (GO), epichlorohydrin (ECH) and 1-ethyl-3-(3-dimethylaminopropyl) carbodiimide (EDC) together with N-hydroxysuccinimide (NHS) and the characteristics of each of them evaluated in the presence of model electroactive compounds potassium hexacyanoferrate(III) and hexaammineruthenium(III) chloride. Immobilisation of functionalised carbon nanotubes into chitosan matrices (Chit–CNT) using the same crosslinking agents was also investigated. The impedance of the electrode with the best performance (GrEC/Chit–CNT/EDC–NHS) was characterised as a sensor for dipyrone and hydroquinone and for a glucose biosensor by immobilisation of glucose oxidase (GOx) on top of Chit–CNT using GA. Modelling and equivalent circuit analysis was carried out, with emphasis on diffusion characteristics and the significant features of the spectra are discussed.

1. Introduction

Electrochemical impedance spectroscopy (EIS) has been used in many fields, particularly corrosion, but only, since the 1980, has it become more widely applied, first to ion-selective electrodes [1] and then, more recently, to electrochemical sensors and biosensors in general [2–5]. The impedance experiments are now easy to perform with modern computer-controlled instrumentation. Nevertheless, good experimental protocols with an assessment of errors and reproducibility, and interpretation and modelling of the spectra, are difficult so that the spectra are often used, in the chemical sensors' field, more for diagnostic characterisation. Despite this apparent limitation, differences between sensing electrode structures can be assessed in a way that is not possible by voltammetric techniques such as cyclic voltammetry or pulse voltammetry, due to the wide range of timescales probed by EIS. Full interpretation of the impedance spectra of sensor systems often requires that the molecular arrangement and structure at the electrode surface or modified surface is predefined or organized in some way, thus avoiding non-uniformity at the nanoscale [6].

Many types of electrochemical sensor and biosensor assembly have been the object of research. Particularly interesting sensor architectures include modifiers which can interact chemically with proteins, such as enzymes, and also with substrate electrode surfaces. Amongst these, chitosan has been shown to have interesting properties. Chitosan (Chit) is a linear β-1,4-linked polysaccharide (similar to cellulose) that is obtained by the partial deacetylation of chitin, a main component of the shells of crustaceans such as crab and shrimp. Chit possesses distinct chemical and biological properties [7], because it has reactive amino and hydroxyl groups in its linear high molar mass polyglucosamine chains which are amenable to chemical modification [8–11]. Moreover, Chit is biocompatible, biodegradable, and is a non-toxic, natural and high mechanical strength biopolymer with an excellent film-forming ability and is also a very good matrix for enzyme or biomacromolecule immobilisation [8].

Carbon nanotubes (CNTs) are often used in sensors and biosensors due to their chemical and mechanical properties. CNTs have good conductivity due to defects in their structure and promote electron transfer reactions of various molecules; their use as electrode modifiers can lead to a decrease of the overpotential, a decrease of the electrode response time, and an increase of the available electroactive surface area of various electroactive substances, in comparison with conventional carbon electrodes [12–21]. Nevertheless, the low solubility of CNTs in most solvents is the major problem to control for their use as modifiers in the fabrication of chemical sensors and/or biosensors. The strategies most employed to disperse CNTs are: (i) functionalisation [16,21,22], (ii) use of surfactants with sonication [23], and (iii) polymer wrapping [24].

* Corresponding author. Tel.: +351 239835295; fax: +351 239835295.
E-mail address: brett@ci.uc.pt (C.M.A. Brett).

0013-4686/$ – see front matter © 2009 Elsevier Ltd. All rights reserved.
doi:10.1016/j.electacta.2009.09.055

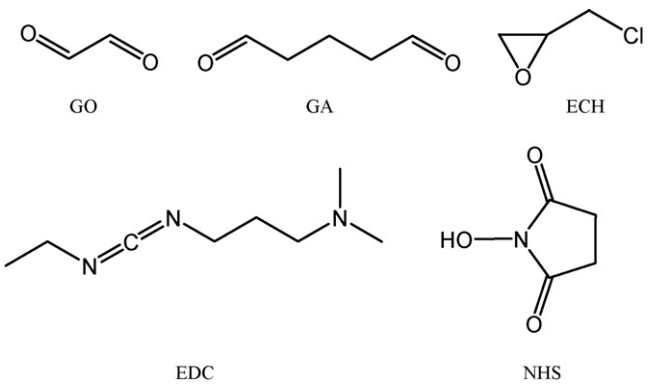

Fig. 1. Chemical structures of glyoxal (GO), glutaraldehyde (GA), epichlorohydrin (ECH), 1-ethyl-3-(3-dimethylaminopropyl) carbodiimide (EDC), and N-hydroxysuccinimide (NHS).

In the present work, electrochemical impedance spectroscopy was used in order to characterise graphite-epoxy resin composite (GrEC) electrodes modified with chitosan films crosslinked with glutaraldehyde (GA), glyoxal (GO), epichlorohydrin (ECH), and 1-ethyl-3-(3-dimethylaminopropyl) carbodiimide (EDC) together with N-hydroxysuccinimide (NHS) (EDC–NHS), structures shown in Fig. 1. The immobilisation of functionalised carbon nanotubes into chitosan matrices using the four crosslinkers was also evaluated. The best electrode composition (GrEC/Chit–CNT/EDC–NHS) was further applied to sensor and biosensor development and tested by EIS with different analytes, hydroquinone, dipyrone, and glucose. Equivalent circuit fitting was mostly carried out with the inclusion of finite Warburg diffusion elements, to reflect the shape of the spectra, and has been done in some recent diagnostic analysis of CNT-based biosensors. Characteristics of the sensors and biosensors developed are discussed.

2. Experimental

2.1. Apparatus

Electrochemical impedance measurements were carried out using a Solartron 1250 Frequency Response Analyser, coupled to a Solartron 1286 Electrochemical Interface (UK) controlled by ZPlot software. The voltage perturbation was 10 mV rms over a frequency range from 65 kHz to 0.1 Hz with 10 frequencies per decade, and integration time 60 s.

A three-electrode electrochemical cell was used for the measurements with graphite-epoxy composite, bare and/or modified, working electrode, Pt foil as auxiliary electrode and saturated calomel electrode (SCE) as reference.

The pH measurements were done with a CRISON 2001 micro pH-meter (Spain).

All experiments were performed at room temperature, 25 + 1 °C.

2.2. Chemicals

Multi-walled carbon nanotubes (MWCNTs) were obtained from NanoLab (USA). Araldit epoxy resin and Araldit hardener were purchased from Ceys S.A. (Spain). Graphite powder (grade #38) was obtained from Fisher Scientific Corporation (USA). Chitosan (Chit) of low molecular weight with a degree of deacetylation of 80%, glucose oxidase (GOx; E.C. 1.1.3.4) from *Aspergillus niger*, type II, lyophilized powder, 15,000–25,000 units/g solid, and α-D(+)glucose were obtained from Aldrich (Germany). Glyoxal (GO) (40%, v/v solution) and epichlorohydrin (ECH) (99%, v/v solution) were obtained from Aldrich (Germany). Glutaraldehyde (GA) (25%, v/v solution), 1-ethyl-3-(3-dimethylaminopropyl) carbodiimide (EDC) were purchased from Sigma (Germany) and N-hydroxysuccinimide (NHS) was from Fluka (Germany). Potassium hexacyanoferrate(III) was acquired from Merck (Germany) and potassium chloride was from Fluka (Germany). Hexaammineruthenium(III) chloride was acquired from Merck (Germany). Millipore Milli-Q nanopure water (resistivity >18 MΩ cm) was used for the preparation of all solutions.

For electrochemical experiments the supporting electrolyte was sodium phosphate buffer saline (NaPBS) (0.1 M Na_2HPO_4/NaH_2PO_4 + 0.05 M NaCl) pH 7.0 or 0.1 M KCl.

2.3. Pretreatment of multi-walled carbon nanotubes

Multi-walled carbon nanotubes (MWCNTs) were purified and functionalised as described elsewhere [16]. A mass of 120 mg of MWCNT was stirred in 10 mL of a 3 M nitric acid solution for 20 h. The solid product was collected on a filter paper and washed several times with nanopure water until the filtrate solution became neutral (pH ≅ 7). The functionalised MWCNTs obtained were then dried in an oven at 80 °C for 24 h. Nitric acid usually causes significant destruction of carbon nanotubes and introduces –COOH groups at the ends or at the sidewall defects of the nanotube structure.

2.4. Preparation of graphite-epoxy composite electrode

Graphite-epoxy composite electrodes were used as electrode substrates. These were prepared using graphite powder and Araldit epoxy resin/hardener by hand-mixing in the ratio 70:30 (m/m), as described previously [25]. The resulting paste was placed into the tip of a 1 mL insulin plastic syringe, and a copper rod with diameter equal to the inner size of the syringe was inserted to give external electrical contact. The resulting electrodes had 5 mm diameter, geometric area 0.196 cm^2, and their thickness was 5–7 mm. Before each use, the surface of the composite electrode was wetted with Milli-Q water and then thoroughly smoothed, first with abrasive paper and then with polishing paper, Kemet (UK).

2.5. Preparation of the film electrodes containing functionalised MWCNTs

A 1.0% m/m Chit stock solution was prepared by dissolving 100 mg of Chit powder in 10 mL of 1.0% (v/v) acetic acid solution and stirred for 3 h at room temperature until complete dissolution. The Chit solution was stored under refrigeration at 4 °C when not in use.

A dispersion of 1.0% m/v functionalised MWCNTs in 1.0% m/m chitosan was prepared by sonication of 2 mg of functionalised MWCNTs in 200 μL of 1.0% m/m Chit in 1.0 % (v/v) acetic acid solution for 2 h.

All chitosan-containing films were obtained using either 1.0% m/m Chit solution or 1.0% m/v functionalised MWCNTs in 1.0% m/m chitosan together with one of the crosslinkers placed directly onto the graphite-epoxy composite electrode; the detailed procedure is given elsewhere [26]. Briefly, the graphite-epoxy composite electrode was covered, in all cases, by first dropping 10 μL of 1% m/m Chit or 10 μL of 1% m/v MWCNTs in 1.0% m/m Chit and leaving it to dry for 1 h. After solvent evaporation, a second aliquot of 10 μL of Chit or MWCNT/Chit dispersion was dropped on the surface and the coated electrode was again left for solvent evaporation at room temperature in air for approximately 1 h. Then, 10 μL of 0.02 M NaOH solution was placed on the surface and dried for 40 min, followed by another aliquot of the same reagent, the purpose being to deprotonate the amino groups of Chit by changing the pH at the electrode surface. In the case of the EDC–NHS crosslinker, this procedure with NaOH solution was performed only once in

order to neutralize the medium at the electrode surface avoiding an increase pH value more than 7. The electrode was washed thoroughly with phosphate buffer solution.

After this, the crosslinker was incorporated by dropping 10 μL of one of the following solutions on the surface: (a) 2.0% (v/v) of GO solution in buffer, (b) 2.5% (v/v) GA solution in buffer, (c) 2.5% (v/v) ECH in 0.1 M NaOH solution (pH 10) and (d) 0.5% (m/v) EDC/0.5% (m/v) NHS solution in buffer. The assemblies were left to dry for 2 h before use.

The electroactive area of each electrode was determined experimentally from the cyclic voltammetry of potassium hexacyanoferrate(III), as described in [27].

2.6. Enzyme immobilisation

Glucose oxidase was immobilised on top of the electrodes previously modified as described above. The electroactive area of the electrodes was $0.64 \pm 0.10\,cm^2$. Volumes of 10 μL of 1% (m/v) GOx, 5 μL of 2.5% (m/v) BSA and 5 μL of 2.5% (v/v) GA were mixed carefully with a thin glass rod directly on top of the electrode and left to react for 1 h. Before use, the excess of GA was washed out with 20 μL of phosphate buffered saline (pH 7.0).

2.7. Analysis of impedance spectra

Impedance spectra were analysed by fitting to equivalent electrical circuits using ZView software (Scribner Associates, USA). All of these included a Warburg element, Z_W, which was modelled as an open circuit finite Warburg element, as already used for other CNT-modified electrodes [28]. The circuits are shown in Fig. 2 and will be referred to and the meaning of the modelling explained within the results and discussion section.

The basic elements are the cell resistance, R_Ω, composed of the solution and the bulk composite resistances, in series with different combinations. The constant phase element, CPE, was modelled as a non-ideal capacitor:

$$\mathrm{CPE} = \frac{-1}{(Ci\omega)^{\alpha}} \quad (1)$$

where the capacitance C describes the charge separation at the double layer interface and the α exponent is due to the heterogeneity of the surface. R_{ct} is the charge transfer resistance.

The definition of the Warburg element used is

$$Z_W\ (W_o) = \frac{R_{dif} ctnh([i\tau\omega]^{\alpha})}{(i\tau\omega)^{\alpha}} \quad (2)$$

where R_{dif} is a diffusion resistance of electroactive species, τ a time constant depending on the diffusion rate ($\tau = l^2/D$, where l is the effective diffusion thickness, and D is the effective diffusion coefficient of the species), and $\alpha = 0.5$ for a perfect uniform flat interface. At "high" frequencies the impedance behaviour is that of infinite diffusion (phase angle 45°) and at "low" frequencies it tends to that of a capacitor (phase angle 90°). Values of α of less than 0.5 express the fact that the interface is not uniform (as happens with CPE non-ideal capacitance when $\alpha < 1$).

3. Results and discussion

3.1. Electrochemical impedance of different crosslinking agents for chitosan–MWCNT cast on the electrode surface

Electrodes were prepared from GrEC and chitosan with and without carbon nanotubes using four different crosslinkers: GO, GA, ECH and EDC–NHS, see structures in Fig. 1, and the crosslinking mechanisms are described in previous work [26]. GO and GA bind covalently with amino groups from Chit releasing water; ECH

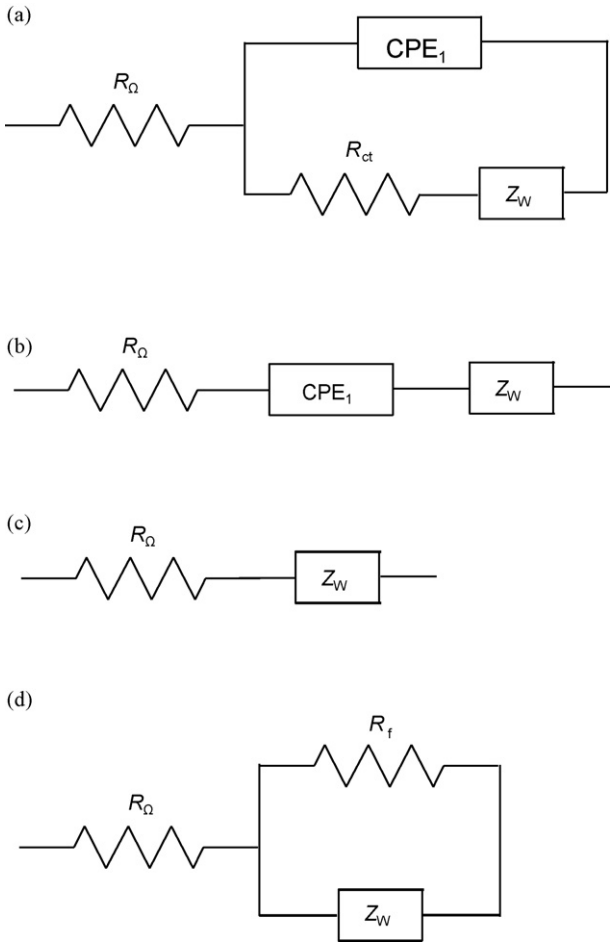

Fig. 2. Equivalent electrical circuits used to fit the impedance spectra. R_Ω is the cell resistance, CPE_1 a constant phase element modelled as a non-ideal capacitor, R_{ct} the charge transfer resistance, R_f a film resistance and Z_W a Warburg impedance modelled as an open finite Warburg element W_o. See text for details.

binds covalently with hydroxyl groups from Chit releasing water and chloride anion. EDC–NHS has a more complex crosslinking mechanism and acts like a catalyst: EDC first covalently attaches to the –COOH groups present on the surface of the graphite-epoxy composite electrode, which then reacts with NHS, substituting EDC, covalently attaching to the functionalised electrode surface whilst releasing 1-(3-dimethylamino)propyl-3-ethylurea. Furthermore, such structures facilitate Chit reaction in which it substitutes NHS, in this way covalently "gluing" the electrode surface with Chit amino groups, releasing unchanged NHS.

EIS was used to shed light on the influence of the different crosslinking agents and of incorporating MWCNT. Impedance spectra were recorded in 3 mM $K_3Fe(CN)_6$ in 0.1 M KCl either at the open circuit potential (OCP), which was in the range +0.15 to +0.25 V depending on the film-modified electrode composition, or fixed at +0.15 V *vs.* SCE. The OCP was close to the midpoint potential from CVs [26] in the case of GA and GO, but it was around 50 mV more positive than the midpoint for ECH and EDC–NHS crosslinked MWCNT–chitosan electrodes. Spectra recorded at OCP and at +0.15 V were similar. The discussion below will focus on spectra recorded at +0.15 V because at fixed potential it is easier to control the redox processes at different electrodes.

In all cases, the spectra obtained include two regions: a semicircular part at high frequencies corresponding to the electron transfer process and a linear part at lower frequencies corresponding to diffusion control (Fig. 3). For the electrodes without MWCNT, i.e. with only chitosan and crosslinkers, the semicircle is not so well defined,

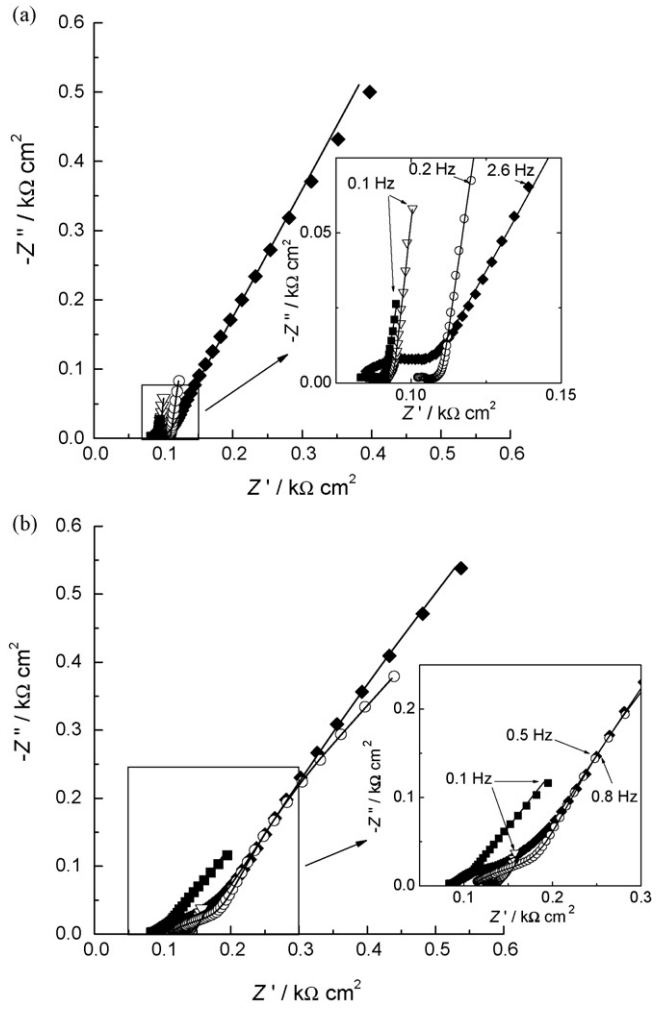

Fig. 3. Complex plane impedance spectra of graphite composite electrodes with chitosan (a) with and (b) without carbon nanotubes with different crosslinkers: (■) EDC–NHS; (♦) GO; (○) GA; (▽) ECH at OCP in 3 mM $K_3Fe(CN)_6$ and 0.1 M KCl. Lines indicate fitting using the equivalent circuit in Fig. 2a.

suggesting that electron transfer is partially blocked by the porous chitosan polymer, see Fig. 2b, as was observed previously [29].

Spectra were fitted using the Randles-type equivalent electrical circuit in Fig. 2a. The high frequency region of the spectra, which represents the charge transfer and charge separation within the various types of Chit film, was analysed in more detail. The values of R_Ω were slightly different for each type of film: ~80 (EDC–NHS), ~85 (GO), ~100 (ECH) and ~115 Ω cm^2 (GA). After modification with MWCNT a small decrease in the R_Ω values was observed. These differences can be explained by the fact that each crosslinker forms a different film structure, which is also changed in the presence of MWCNTs in the film.

The values of the charge transfer resistance decreased significantly with almost all crosslinkers (except GO) when including nanotubes, see Table 1, as would be expected when the MWCNT cause an electrocatalytic effect. The capacitance values increased in all cases with the addition of carbon nanotubes due to an increase in the electroactive area of the electrode, showing easier electron transfer in the presence of MWCNT within the Chit-crosslinker modified films. The lowest charge transfer resistance values were obtained for ECH followed by EDC–NHS, GA, and finally GO, meaning that at ECH and EDC–NHS crosslinked MWCNT–Chit films the electron transfer is facilitated. This is in agreement with cyclic voltammetry where the best crosslinkers were EDC–NHS and ECH:

Table 1
Equivalent circuit fitting data from impedance at carbon nanotubes immobilised into chitosan using different crosslinkers. The spectra were recorded at +0.15 V *vs.* SCE.

Film composition	R_{ct} (Ω cm^2)	C (μF cm^{-2} s^{n-1})	α
CHIT–GO	22	0.04	0.70
CHIT–GO–MWCNT	36	154	0.81
CHIT–GA	91	0.45	0.72
CHIT–GA–MWCNT	17	207	0.89
CHIT–ECH	238	1.9	0.73
CHIT–ECH–MWCNT	4	279	0.74
CHIT–EDC–NHS	50	120	0.85
CHIT–EDC–NHS–MWCNT	12	213	0.89

although the order of EDC–NHS and ECH is changed in the case of EIS, the values of the charge transfer resistance are very close to each other so no clear distinction can be made as to which is better [26].

Electrochemical impedance spectra recorded at bare, chitosan and chitosan-nanotube electrodes, crosslinked with EDC–NHS, in 0.1 M KCl solution, with and without 3.0 mM $Ru(NH_3)_6Cl_3$, at the open circuit potential (OCP), which was ~+0.15 V *vs.* SCE are shown in Fig. 4. The reason for adding the redox couple is that, in the literature, impedance spectra recorded at other types of CNT biosensor-modified electrodes (to be described below in Section 3.2.2) mostly used hexacyanoferrate(II) and ruthenium hexaammine(III) redox couples and measurements at OCP [30–33]. All bare and Chit-modified electrodes exhibited similar behaviour with the impedance values varying about 20% between three equal electrodes (not shown).

Unmodified GrCE exhibited a non-ideal capacitive behaviour over the whole frequency range and the imaginary part of the impedance reached a value of ~12 kΩ cm^2 at 0.1 Hz, as seen in Fig. 4. There was no change in the spectra with and without $Ru(NH_3)_6^{3-}$ at the OCP at this kind of electrode.

The GrEC/Chit electrodes had much lower imaginary impedance values than at the bare GrEC electrode, attributed to an increased interfacial capacitance of the modified electrodes. The spectra demonstrate that both resistivity and electrode surface structure changed with the modification of the graphite-epoxy composite, as expected.

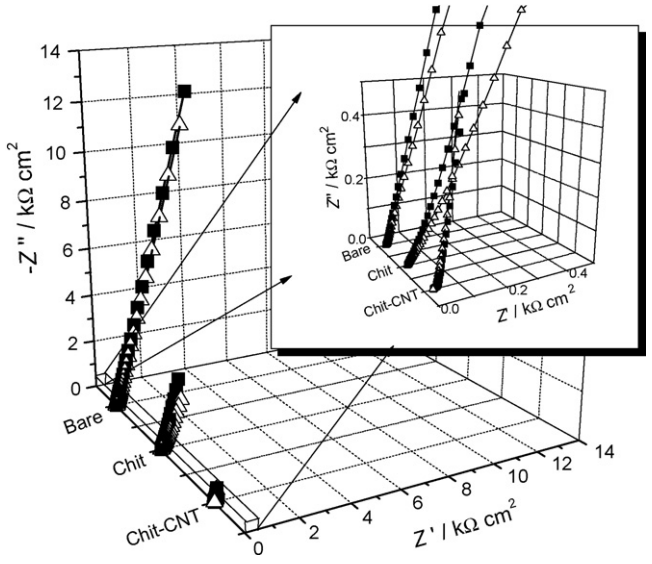

Fig. 4. Complex plane impedance spectra at GrEC, GrEC/Chit, and GrEC/Chit–CNT electrodes at OCP in 0.1 M KCl (■) without and (Δ) with 3 mM $Ru(NH_3)_6Cl_3$. Lines indicate fitting using the equivalent circuits in Fig. 2b for GrEC, GrEC/Chit and in Fig. 2a for GrEC/Chit–CNT electrodes.

Table 2
Parameters from W_o in impedance spectra obtained by equivalent circuit fitting at different electrodes in 0.1 M KCl and with addition of 3.0 mM $Ru(NH_3)_6Cl_3$ at open circuit potential (OCP).

Electrode	Solution composition	C_{dl} ($\mu F\,cm^{-2}$)	R_{ct} ($\Omega\,cm^2$)	R_{dif} (W_o) ($\Omega\,cm^2$)	τ (W_o) (s)	α (W_o)
Bare	Electrolyte	1.95	–	3.2	0.001	0.41
	$+Ru(NH_3)_6^{3+}$	0.82	–	8.3	0.001	0.40
Chit	Electrolyte	1.16	–	3.6	0.001	0.41
	$+Ru(NH_3)_6^{3+}$	2.28	–	16.4	0.009	0.43
Chit–MWCNT	Electrolyte	44.8	16.2	24.6	0.064	0.45
	$+Ru(NH_3)_6^{3+}$	44.8	16.9	21.4	0.060	0.44

The spectra at the GrEC/Chit–MWCNT electrodes were different from those without MWCNT, with a charge transfer semicircle in the high frequency region and a linear diffusion part in the middle and low frequency region. The imaginary impedance value at 0.1 Hz dropped to 0.4 $k\Omega\,cm^2$, again showing an increase in capacitance and the decrease of the real impedance and demonstrating an increase in conductivity of these electrodes after modification with MWCNTs.

Almost all spectra could be fitted to a circuit consisting of a cell resistance in series with a constant phase element (CPE) and a finite Warburg element (W_0): $-R_\Omega$–CPE–W_o– for the spectra without CNT (Fig. 2b, bare composite electrode and modified with chitosan) and a Randles-type equivalent circuit (Fig. 2a, as above) for the MWCNT-modified electrodes. The CPE describes a capacitance which increases with chitosan modification. The different circuit for the GrEC/Chit–MWCNT is a reflection of the fact that the some pathways to the electrode substrate include MWCNT in parallel with others that do not. Data from analysis of the impedance spectra are presented in Table 2. Apart from the considerations made above, they show that the charge separation is much larger in the presence of MWCNT, the diffusion resistance of an electroactive species through the chitosan matrix is also much higher as well as the Warburg time constant. There is some effect of the ruthenium cationic species on the charge separation in Chit-modified electrodes.

The impedance results show that modification of graphite-epoxy composite with CNTs attached to the electrode surface by crosslinked chitosan have much better characteristics for application as sensors than unmodified electrodes.

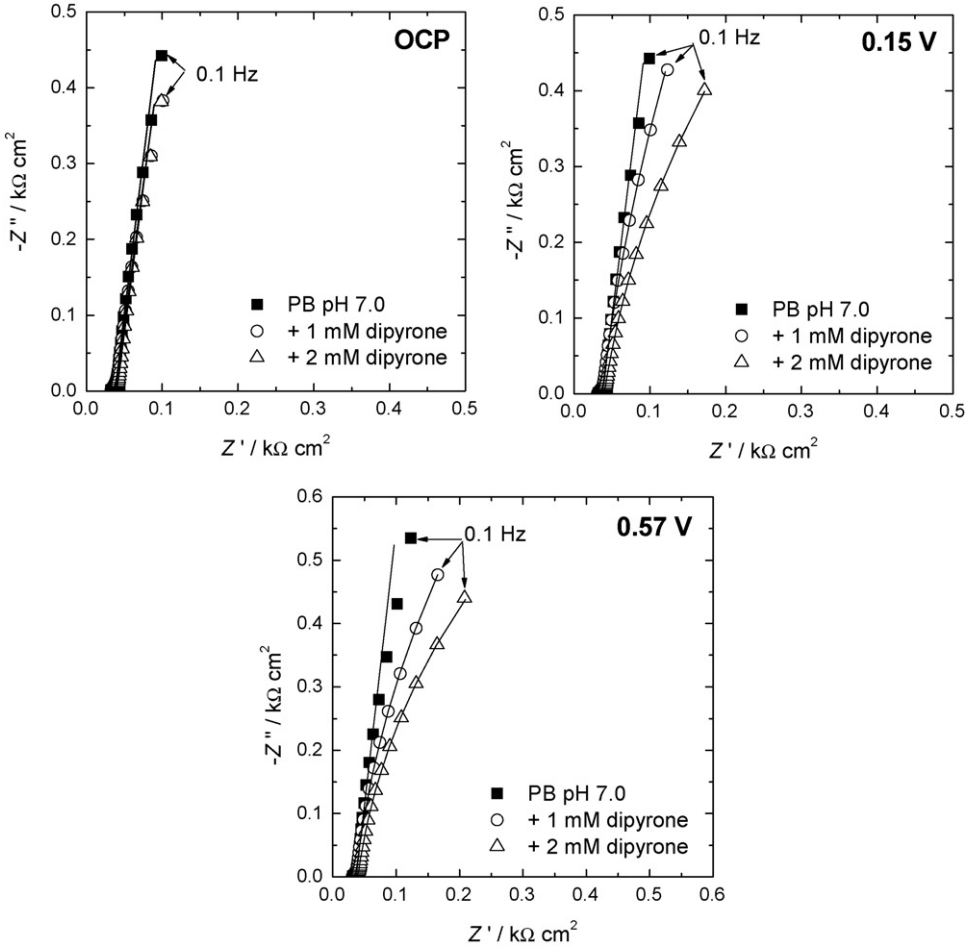

Fig. 5. Complex plane impedance spectra at GrEC/Chit–CNT–EDC–NHS sensor at different potentials in 0.1 M NaPBS pH 7.0, in the presence and absence of dipyrone. OCP was ~20 mV *vs.* SCE. Lines indicate fitting using the equivalent circuit in Fig. 2c at OCP and 0.15 V without dipyrone and in Fig. 2d for all the other spectra.

Table 3
Equivalent circuit fitting of impedance data at carbon nanotubes immobilised into chitosan using EDC–NHS as crosslinker in 0.1 M phosphate buffer, pH 7.0 with and without dipyrone (dipy). OCP was ~20 mV *vs.* SCE.

E (V *vs.* SCE)	Solution composition	R_{dif} (W_o) (Ω cm^2)	τ (W_o) (s)	α (W_o)	R_f (kΩ cm^2)
OCP	Buffer	18	0.063	0.46	–
	+1 mM dipy	17	0.053	0.46	–
	+2 mM dipy	18	0.054	0.46	–
0.15	Buffer	19	0.051	0.46	–
	+1 mM dipy	18	0.048	0.46	5.9
	+2 mM dipy	17	0.043	0.45	2.4
0.57	Buffer	19	0.044	0.47	7.8
	+1 mM dipy	17	0.040	0.46	3.2
	+2 mM dipy	17	0.038	0.46	2.0

3.2. Investigation of sensors and biosensor based on Chitosan–MWCNT–EDC–NHS

3.2.1. Chitosan–MWCNT–EDC–NHS sensors for dipyrone and hydroquinone

As found above, the best crosslinking agent for application of the Chit–CNT-modified electrode is EDC–NHS [26], so the performance of Chit–MWCNT–EDC–NHS was tested by EIS in phosphate buffer. The electrode was applied to the determination of some important analytes, exemplified here by dipyrone and hydroquinone. Spectra were also recorded in the absence and presence of these compounds in order to examine electrode performance in the presence of analyte.

Fig. 5 presents complex plane impedance spectra at different potentials in 0.1 M phosphate buffer solution, pH 7.0, and with the addition of 1 and 2 mM dipyrone at different potentials, where the most pronounced oxidation peaks of dipyrone were found (0.15 and 0.57 V [34]) and at OCP, which was ~0.02 V *vs.* SCE. At OCP, where no peaks occur in cyclic voltammetry, no changes were obtained in the complex plane spectra on addition of analyte. However, at the other potentials studied, the spectra had lower impedance values in the low frequency region after dipyrone addition, showing the lower diffusion resistance with each addition of aliquot of 1 mM dipyrone to the buffer solution. Nevertheless, only small changes were obtained in the high frequency region.

The spectra at OCP and at 0.15 V (the latter without dipyrone addition), were best fitted just with R_Ω and open Warburg element, W_o, in series (Fig. 2c). However, the spectra at 0.15 and 0.57 V, after addition of dipyrone (at 0.57 V even without addition of analyte) lost their linearity in complex plane plots (Fig. 5) and so at these potentials a film resistance, R_f, was added in parallel with W_o reflecting the duplex nature of the film in that only parts of it have active sites available for reaction (Fig. 2d). The values of the parameters from equivalent circuit analysis are presented in Table 3. R_Ω was $31 \pm 2\,\Omega\,cm^2$ at all potentials studied in buffer without and with dipyrone. As expected, the Warburg element values changed with addition of dipyrone. R_{dif} changes slightly and decreases by 1–2 Ω cm^2 with analyte addition showing slightly faster diffusion; τ decreases with each addition of analyte; and the exponent α also decreases with addition of dipyrone. The film resistance, R_f, also decreases with increase of dipyrone concentration, showing that the analyte increases diffusion of the charged species, counter ions or dipyrone oxidation products, through the porous film as well as the area through which this occurs.

Spectra were recorded with the same electrode in pH 4.1 0.1 M acetate buffer in the presence of 1 mM hydroquinone at OCP (~+0.15 V *vs.* SCE) and at +0.2 V *vs.* SCE, shown in Fig. 6 in complex plane plots. The spectra obtained were different: at +0.2 V a semicircle part and a linear part are seen, as reported above (see Section 3.1), whilst at OCP no semicircle was observed. The spectra were fitted using two different circuits: at OCP a cell resistance R_Ω in series with a Warburg element W_o (no electrode reaction, Fig. 2c) and at +0.2 V a Randles circuit was necessary (Fig. 2a) with a pure capacitance rather than a CPE. The values of parameters obtained from fitting at +0.2 V showed almost the same value of the cell resistance, as expected (~75 Ω cm^2), and the value of R_{ct} is very small (5.5 Ω cm^2); the value of C_1 was 140 μF cm^{-2}.

These results demonstrate the potentialities of EIS for the characterisation of such types of modified electrode structure used as sensors and can lead to quantitative determination protocols for different analytes. Additionally, it demonstrates the different interactions of analytes at the modified electrode surfaces, shown here by the different equivalent circuits needed for fitting the experimental data.

3.2.2. Chitosan–MWCNT–EDC–NHS/GOx biosensor

Impedance spectra were recorded at GrEC/Chit–CNT/GOx biosensors at different potentials, 0.1, 0.0, −0.1, −0.3, and −0.45 V, in the region where H_2O_2 reduction, O_2 reduction and FAD/FADH$_2$ redox processes take place [35], and which are therefore of interest for biosensor functioning, in the presence and absence of dissolved oxygen in the buffer solution. These spectra are presented in Fig. 7a and show that there was no significant difference between them in

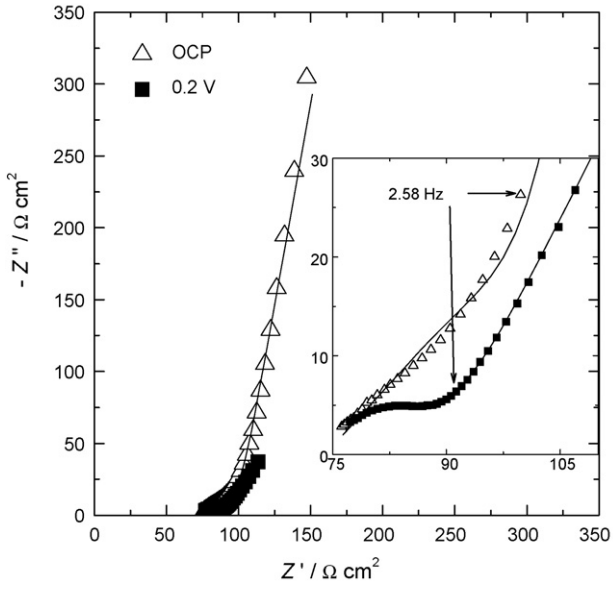

Fig. 6. Complex plane impedance spectra at GrEC/Chit–CNT–EDC–NHS sensor at OCP (~0.15 V) (△) and 0.2 V (■) *vs.* SCE in 0.1 M acetate buffer pH 4.1, in the presence of 1 mM hydroquinone. Lines indicate fitting using the equivalent circuit in Fig. 2c at OCP and in Fig. 2a at +0.15 V.

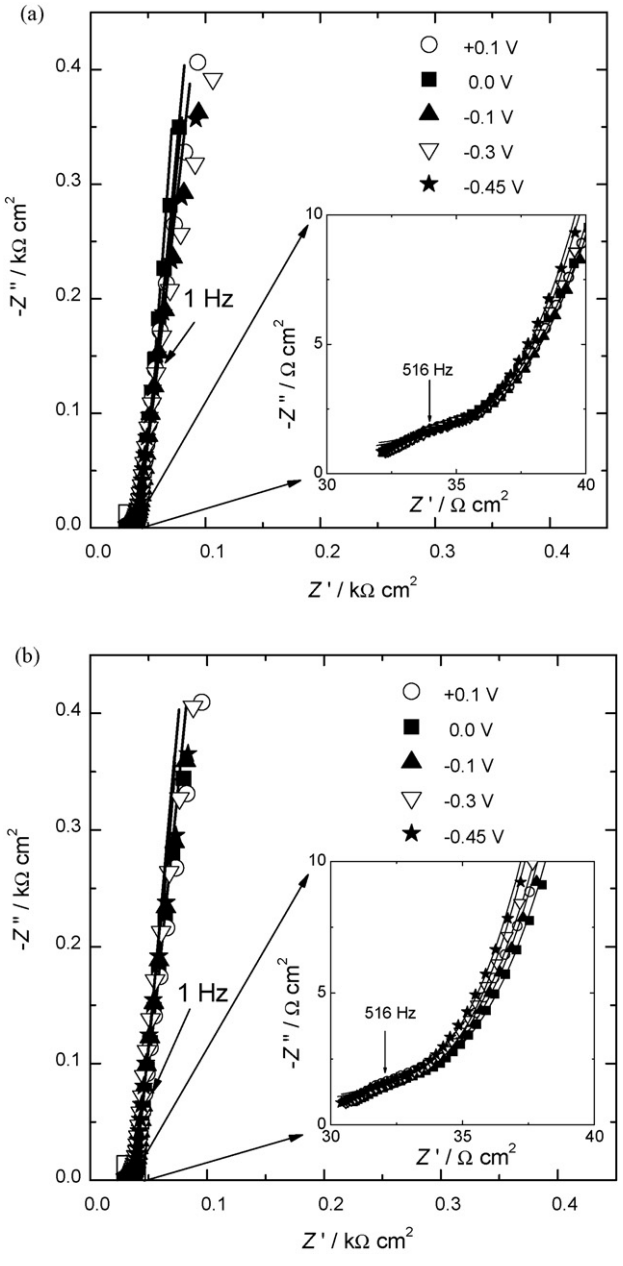

Fig. 7. Complex plane impedance spectra at GrEC/Chit–CNT/GOx biosensor at different potentials in 0.1 M NaPBS pH 7.0: (a) before and (b) after oxygen removal. Lines indicate fitting using the equivalent circuit in Fig. 2c.

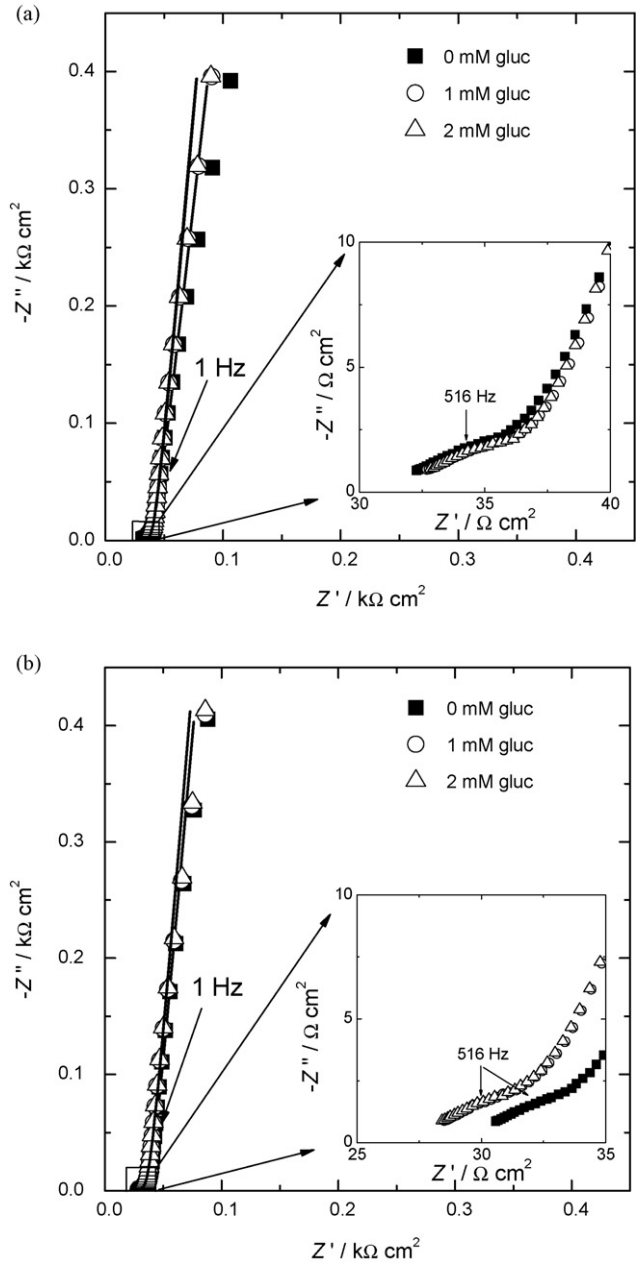

Fig. 8. Complex plane impedance spectra at GrEC/Chit–CNT/GOx biosensor at −0.3 V *vs.* SCE (a) with and (b) without dissolved O_2 in 0.1 M NaPBS, pH 7.0, in the absence and presence of 1 and 2 mM of glucose. Lines indicate fitting using the equivalent circuit in Fig. 2c.

this potential region. Deoxygenation of the buffer solution shifted the impedance to lower values in the high frequency region but did not introduce any other changes in the low frequency region (Fig. 7b). These results, obtained with and without dissolved oxygen in solution, lead to the conclusion that dissolved oxygen affects the biosensor characteristics, as expected.

In order to study biosensor performance, impedance spectra were also recorded after the addition of glucose to the buffer solution, under the same conditions as without glucose, including also in deoxygenated solutions, see Fig. 8. Addition of 1 mM glucose to the buffer solution slightly decreased the values of imaginary impedance and the real part of impedance became very slightly higher in the high frequency region (Fig. 8a, inset) having an opposite effect in the region of low frequency. The same shift was observed after addition of a further 1 mM of glucose; however, this shift was smaller than the previous one. This was probably because of saturation of the biosensor, since the linear range of the biosensor was up to 0.8 mM [35].

In the deoxygenated buffer solution the behaviour was essentially the same as in the presence of oxygen: the same shift in the impedance values were observed in the low frequency region after addition of 1 mM of glucose and in the high frequency region the spectrum is shifted closer to zero; no significant changes was observed after addition of another aliquot of 1 mM glucose These results lead to the conclusion that oxygen might be trapped in the biosensor membrane or in the composite electrode itself.

The equivalent circuit in Fig. 2c was used to fit all spectra, i.e. R_Ω in series with W_o. The cell resistance had a value of $30 \pm 2\,\Omega\,cm^2$ at all potentials, in the presence and absence of oxygen in buffer solution. It decreases $1–2\,\Omega\,cm^2$ after the first glucose addition

Table 4
Parameters from W_o in impedance spectra obtained by equivalent circuit fitting at GrEC/Chit–CNT/GOx-modified electrodes in 0.1 M NaPBS in the presence and absence of dissolved oxygen at −0.1, −0.3, and −0.45 V *vs.* SCE.

E (V *vs.* SCE)	Solution	R_{dif} (W_o) (Ω cm^2)	τ (W_o) (s)	α (W_o)
Presence of O_2				
−0.1	Buffer	23	0.078	0.46
	+1 mM gluc	21	0.075	0.46
	+2 mM gluc	20	0.073	0.46
−0.3	Buffer	21	0.063	0.46
	+1 mM gluc	20	0.062	0.46
	+2 mM gluc	20	0.061	0.47
−0.45	Buffer	21	0.071	0.46
	+1 mM gluc	20	0.067	0.46
	+2 mM gluc	19	0.066	0.46
Absence of O_2				
−0.1	Buffer	21	0.072	0.46
	+1 mM gluc	21	0.073	0.46
	+2 mM gluc	21	0.072	0.46
−0.3	Buffer	20	0.061	0.47
	+1 mM gluc	21	0.062	0.48
	+2 mM gluc	21	0.061	0.47
−0.45	Buffer	20	0.066	0.46
	+1 mM gluc	20	0.067	0.46
	+2 mM gluc	20	0.067	0.46

and then remains constant in the absence of oxygen, however, it usually remained constant after glucose addition in the solutions with O_2. The equivalent circuit parameters obtained at different potentials in the presence and absence of oxygen and glucose are presented in Table 4. Analysis of the impedance data demonstrates that almost no changes are observed at the electrode surface after glucose addition in the absence of O_2. However, in the presence of oxygen resistance of diffusion and factor τ, related to the diffusion time, decreased slightly with addition of analyte to the buffer solution.

Impedance spectra recorded at other types of CNT biosensor-modified electrodes at OCP, had a similar profile to those reported in this work and were analysed using the Randles equivalent electrical circuit [30–33].

The impedance data demonstrated that the electrode surface does not change with applied potential but does change slightly with the presence or absence of oxygen and almost not at all in the presence of the enzyme substrate, glucose. This type of sensing architecture, which is an extremely promising alternative as a biosensor [26,34] shows the desirable criterion of not altering its characteristics when functioning in the presence of the analyte.

4. Conclusions

Electrochemical impedance spectroscopy was used to characterise chitosan-modified electrodes with different crosslinkers regarding their effectiveness together with the immobilisation of functionalised MWCNT in different aqueous media. Successful modelling of the spectra was based on the use of diffusional elements for the different modified electrode structures. The electrode modified with chitosan and carbon nanotubes using EDC–NHS crosslinker was sensitive to changes in dipyrone and hydroquinone analyte concentration and EIS can be used to obtain information about the behaviour resulting from the film modification. With an external glucose oxidase layer, EIS shows that the glucose biosensor characteristics remain the same in the presence of the enzyme substrate, which augurs well for application of this biosensor architecture.

Acknowledgements

Financial support from Fundação para a Ciência e a Tecnologia (FCT), PTDC/QUI/65255/2006 and PTDC/QUI/65732/2006, POCI 2010 (co-financed by the European Community Fund FEDER) and CEMUC® (Research Unit 285), Portugal, is gratefully acknowledged. O.F.F. thanks CAPES/4383-07-9, UFSCar and the University of Coimbra for a visiting professorship. R.P. and M.E.G. thank FCT for postdoctoral fellowships SFRH/BPD/27075/2006, and SFRH/BPD/36930/2007, respectively.

References

[1] G. Horvai, E. Gráf, K. Tóth, E. Pungor, R.P. Buck, Anal. Chem. 58 (1986) 2735.
[2] B. Pejcic, R. de Marco, Electrochim. Acta 51 (2006) 6217.
[3] I.I. Suni, Trends Anal. Chem. 27 (2008) 604.
[4] C.M.A. Brett, ECS Trans. 13 (13) (2008) 67.
[5] B. Piro, J. Haccoun, M.C. Pham, L.D. Tran, A. Rubin, H. Perrot, C. Gabrielli, J. Electroanal. Chem. 577 (2005) 155.
[6] C.M.A. Brett, S. Kresak, T. Hianik, A.M. Oliveira Brett, Electroanalysis 15 (2003) 557.
[7] H. Yi, L.Q. Wu, W.E. Bentley, R. Ghodss, G.W. Rubloff, J.N. Culver, G.F. Payne, Biomacromolecules 6 (2005) 2881.
[8] I.R.W.Z. de Oliveira, I.C. Vieira, Enzyme Microb. Technol. 38 (2006) 449.
[9] Y. Wan, K.A.M. Creber, B. Peppley, V.T. Bui, Polymer 44 (2003) 1057.
[10] Y. Deng, D. Liu, G. Du, X. Li, J. Chen, Polym. Int. 56 (2007) 738.
[11] J. Cruz, M. Kawasaki, W. Gorski, Anal. Chem. 72 (2000) 680.
[12] L. Agüí, P. Yáñez-Sedeño, J.M. Pingarrón, Anal. Chim. Acta 622 (2008) 11.
[13] G.G. Wildgoose, C.E. Banks, H.C. Leventis, R.G. Compton, Microchim. Acta 152 (2006) 187.
[14] C.E. Banks, R.G. Compton, Analyst 130 (2005) 1232.
[15] C.E. Banks, R.G. Compton, Analyst 131 (2006) 15.
[16] C. Gouveia-Caridade, R. Pauliukaite, C.M.A. Brett, Electrochim. Acta 53 (2008) 6732.
[17] J. Wang, M. Li, Z. Shi, N. Li, Z. Gu, Anal. Chem. 74 (2002) 1993.
[18] G.C. Zhao, Z.Z. Yin, L. Zhang, X.W. Wei, Electrochem. Commun. 7 (2005) 256.
[19] Y.J. Yin, P. Wu, Y.F. Lu, P. Du, Y.M. Shi, C.X. Cai, J. Solid. State Electrochem. 11 (2007) 390.
[20] Q. Zhao, Z.H. Gan, Q.K. Khuang, Electroanalysis 14 (2002) 1609.
[21] R.K. Saini, I.W. Chiang, H.Q. Peng, R.E. Smalley, W.E. Billups, R.H. Hauge, J.L. Margrave, J. Am. Chem. Soc. 125 (2003) 3617.
[22] J. Chen, M.A. Hamon, H. Hu, Y. Chen, A.M. Rao, P.C. Eklund, R.C. Haadon, Science 282 (1998) 95.
[23] M.F. Islam, E. Rojas, D.M. Bergey, A.T. Johnson, A.G. Yodh, Nano Lett. 3 (2003) 269.
[24] A. Star, J.F. Stoddart, D. Steuerman, M. Diehl, A. Boukai, E.W. Wong, X. Yang, S.W. Chung, H. Choi, J.R. Heath, Angew. Chem. Int. Ed. 40 (2001) 1721.

[25] R.L.R.P. Fagury, K.O. Lupetti, O. Fatibello-Filho, Anal. Lett. 38 (2005) 1857.
[26] R. Pauliukaite, M.E. Ghica, O. Fatibello-Filho, C.M.A. Brett, Anal. Chem. 81 (2009) 5354.
[27] J.J. Gooding, V.G. Praig, E.A.H. Hall, Anal. Chem. 70 (1998) 2396.
[28] J. Pillay, K.I. Ozoemena, Electrochim. Acta 52 (2007) 3630.
[29] A. Salimi, H. MamKhezria, R. Hallaj, S. Zandi, Electrochim. Acta 52 (2007) 6097.
[30] X. Kang, Z. Mai, X. Zou, P. Cai, J. Mo, Talanta 74 (2008) 879.
[31] X. Chen, J. Chen, C. Deng, C. Xiao, Y. Yang, Z. Nie, S. Yao, Talanta 76 (2008) 763.
[32] S.N. Liu, Y.J. Yin, C.X. Cai, Chin. J. Chem. 25 (2007) 439.
[33] L. Liu, F. Zhang, F. Xi, Z. Chen, X. Lin, J. Electroanal. Chem. 623 (2008) 135.
[34] R. Pauliukaite, M.E. Ghica, O. Fatibello-Filho, C.M.A. Brett, in preparation.
[35] M.E. Ghica, R. Pauliukaite, O. Fatibello-Filho, C.M.A. Brett, Sens. Actuators B 142 (2009) 308.